# Water and Small-Molecule Permeation of Dormant *Bacillus subtilis* Spores

Scott M. Knudsen,[a] Nathan Cermak,[b] Francisco Feijó Delgado,[a] Barbara Setlow,[c] Peter Setlow,[c] Scott R. Manalis[a,b,d]

Departments of Biological[a] and Mechanical[d] Engineering and Program in Computational and Systems Biology,[b] Massachusetts Institute of Technology, Cambridge, Massachusetts, USA; Department of Molecular Biology and Biophysics, UConn Health, Farmington, Connecticut, USA[c]

**ABSTRACT**

We use a suspended microchannel resonator to characterize the water and small-molecule permeability of *Bacillus subtilis* spores based on spores' buoyant mass in different solutions. Consistent with previous results, we found that the spore coat is not a significant barrier to small molecules, and the extent to which small molecules may enter the spore is size dependent. We have developed a method to directly observe the exchange kinetics of intraspore water with deuterium oxide, and we applied this method to wild-type spores and a panel of congenic mutants with deficiencies in the assembly or structure of the coat. Compared to wild-type spores, which exchange in approximately 1 s, several coat mutant spores were found to have relatively high water permeability with exchange times below the ~200-ms temporal resolution of our assay. In addition, we found that the water permeability of the spore correlates with the ability of spores to germinate with dodecylamine and with the ability of $TbCl_3$ to inhibit germination with L-valine. These results suggest that the structure of the coat may be necessary for maintaining low water permeability.

**IMPORTANCE**

Spores of *Bacillus* species cause food spoilage and disease and are extremely resistant to standard decontamination methods. This hardiness is partly due to spores' extremely low permeability to chemicals, including water. We present a method to directly monitor the uptake of molecules into *B. subtilis* spores by weighing spores in fluid. The results demonstrate the exchange of core water with subsecond resolution and show a correlation between water permeability and the rate at which small molecules can initiate or inhibit germination in coat-damaged spores. The ability to directly measure the uptake of molecules in the context of spores with known structural or genetic deficiencies is expected to provide insight into the determinants of spores' extreme resistance.

$S$pores of some *Bacillus* and *Clostridium* species are causative agents of a number of human and animal diseases, as well as food spoilage and food poisoning (1). This is because spores are extremely hardy and can survive mild decontamination procedures that kill growing bacteria. While a number of factors are responsible for spores' high resistance, one factor is their low permeability to many toxic chemicals, in particular chemicals that can damage spore DNA that is located in the central spore core (2–7). There are a number of permeability barriers in the dormant spore. The outermost is the exosporium, found on spores of some but not all species, which prevents permeation by very large molecules (>150 kDa) (8). Moving inward, the second permeability barrier is the spore coat layer and the underlying outer spore membrane (3, 5). It is not clear that the outer membrane remains intact in dormant spores, although older data suggest that there is a permeability barrier just below the coat (4, 9, 10). This coat/outer membrane barrier restricts access of smaller molecules (>2 to 8 kDa) to inner spore regions, in particular the spores' large peptidoglycan cortex just below the outer spore membrane. As a consequence, intact spores and spores with minor coat defects are resistant to peptidoglycan hydrolases such as lysozyme, but spores with severe coat defects are lysozyme sensitive (5, 11).

The final known spore permeability barrier is the inner membrane (IM) surrounding the central spore core. The IM has a lipid composition similar to that in growing/sporulating cells, but lipid probes incorporated into the IM during sporulation are immobile (12, 13). Methylamine, a small molecule that can be accumulated at high levels in spores because of the low core pH, is often used to probe the integrity of the IM because its rate of entry into the spore core is lower than that of water. Indeed, IM permeability to methylamine is very low, and this low permeability is even retained in spores that lack a coat and outer membrane (2, 14, 15). However, damaging the IM with oxidizing agents can significantly increase its permeability to methylamine (16).

The degree to which water is permeable into various compartments of dormant spores is poorly understood. All spore compartments contain water, although the core is thought to be only ~30% water by weight while outer spore layers are ~80% water (17, 18). Water does penetrate through the entire spore core, and there are several reports that rates of water movement across the IM are rather low, as is movement of other small molecules into

TABLE 1 Strains used in this study[a]

| Strain | Genotype (relevant mutation[s]) |
|---|---|
| PS533 | Wild type |
| PS3328 (Tc[r]) | *cotE* |
| PS3634 | *cotXYZ* |
| PS3735 | *spoVID* |
| PS3736 | *cotH* |
| PS3740 (Cm[r]) | *cotE* |
| PS3738 (Tc[r]) | *safA* |
| PS4133 | *cotB* |
| PS4134 | *cotO* |
| PS4149 (Sp[r]) | *gerE* |
| PS4150 (Tc[r] Sp[r]) | *cotE gerE* |
| PS4427 (Cm[r] Tc[r]) | *cotE safA* |

[a] Strains were obtained from sources given in references 24 and 37 or were generated in this work as described in Materials and Methods. Cm[r], resistance to chloramphenicol (5 μg/ml); Tc[r], resistance to tetracycline (10 μg/ml); Sp[r], resistance to spectinomycin (100 μg/ml).

the spore core (1, 18–23). However, other reports suggest that the barrier to water entry into the spore core is not exclusively the IM (4, 9, 10, 22). Therefore, the question of whether the IM truly is the barrier to water entering the spore core remains an open one.

In order to further examine the permeation of water into dormant *Bacillus subtilis* spores, we have quantified the content of spore material and the extent to which small molecules can permeate the spore based on buoyant mass. Buoyant mass, i.e., the weight of a spore in fluid (see equation below), is determined by weighing single spores as they pass through or are trapped within a suspended microchannel resonator (SMR). We have also developed a method to track spores' buoyant mass as their internal $H_2O$ is replaced with heavy water ($D_2O$) and have analyzed this water movement in spores of a number of congenic mutant *B. subtilis* strains with defects in the coat/outer membrane of various levels of severity. Finally, we tested for the permeation of the outer layers of these spores to $Tb^{3+}$ ions and dodecylamine using a germination assay. Interestingly, we found that water permeation measured by the SMR could be used to predict the permeation of $Tb^{3+}$ ions and dodecylamine. Overall, the findings in this work provide new information on the permeation of water and other small molecules into various compartments of a dormant spore and demonstrate that the structure of the coat is important for maintaining low water permeability.

## MATERIALS AND METHODS

**B. subtilis strains used and spore purification.** The wild-type *B. subtilis* strain used in this work was strain PS533 (24), a derivative of strain PS832, a prototrophic laboratory 168 strain; strain PS533 carries plasmid pUB110 providing resistance to kanamycin (10 μg/ml). All other strains are listed in Table 1 and are congenic with strain PS533 but lack plasmid pUB110. Strain PS4427 was constructed by transforming strain PS3738 (*safA* mutant) to a strain with chloramphenicol resistance with DNA from strain PS3740 (*cotE* mutant).

Spores of all strains were prepared at 37°C on 2× Schaeffer's-glucose medium agar plates (25, 26) without antibiotics. Plates were incubated for 2 to 3 days at 37°C and then for 2 to 4 days at 23°C to allow extensive autolysis of sporulating cells and cell debris. The spores were then scraped from plates into cold deionized water, and spores were purified at 4°C over ~7 days by multiple rounds of centrifugation, washing pellets with cold water to remove debris, and with brief sonication between centrifugation to further disrupt debris. Purified spores were stored at 4°C in water pro-

tected from light. All spores used in this work were >98% free of growing or sporulating cells, germinated spores, and cell debris as determined by phase-contrast microscopy.

**Spore germination.** Spores of various strains were germinated with either L-valine or dodecylamine essentially as described previously (27, 28). In all cases, spore germination was monitored by measuring the release of the spore core's large depot (~20% of core dry weight) of dipicolinic acid (DPA) by its fluorescence with $Tb^{3+}$ either by inclusion of $TbCl_3$ in germination solutions or by removal of 180-μl aliquots of germination mixes incubated without $TbCl_3$ and addition of 20 μl of 500 μM $TbCl_3$. Specific germination conditions were as follows. For L-valine germination, spores at an optical density at 600 nm ($OD_{600}$) of 2.0 were first heat activated for 30 min at 75°C and then cooled on ice for at least 10 min. Spores at an $OD_{600}$ of 0.5 were germinated at 37°C in 200 μl of 25 mM K-HEPES buffer (pH 7.4)–50 μM $TbCl_3$–10 mM L-valine, which is a saturating concentration for this germinant. These mixtures were incubated in a multiwell fluorescence plate reader, and Tb-DPA fluorescence was read every 5 min. For analysis of L-valine germination without Tb present throughout germination, 2 to 3 ml germination mixtures under the same conditions as those described above, but without $TbCl_3$, were incubated in a water bath at 37°C; at various times, 180-μl aliquots were added to 20 μl of 500 μM $TbCl_3$, and the fluorescence of the mixture was read immediately as described above.

Dodecylamine germination of spores is not stimulated by heat activation (27) and was carried out in the absence of $TbCl_3$ as described above for L-valine germination, but with 0.8 mM dodecylamine and at 50°C. Again, 180-μl aliquots of germination mixtures were added to 20 μl of 500 μM $TbCl_3$ and the fluorescence was read as described above. The amount of total DPA in all spores used for germination experiments was determined by boiling spores for 30 min, centrifuging, and measuring DPA in the supernatant fluid by its fluorescence with $Tb^{3+}$ as described previously (28, 29). These total DPA values were used to determine the percentages of spore germination in all germination experiments.

**Buoyant mass determination in an SMR.** The SMR is a microfluidic device that consists of a fluid channel embedded in a vacuum-packaged cantilever (30). The cantilever resonates at a frequency proportional to its total mass, and as an individual spore travels through the embedded microchannel, the total cantilever mass changes. This change in mass is detected as a change in resonance frequency that corresponds directly to the buoyant mass of the spore. Buoyant mass ($m_b$) is the weight of the spore in fluid and is equivalent to the mass of the spore in excess of the fluid that it displaces, as shown in the following equation, where $m$, $V$, and $\rho$ are the mass, volume, and density, respectively, of the spore and $\rho_{fluid}$ is the density of the solution: $m_b = V(\rho - \rho_{fluid}) = m[1 - (\rho_{fluid}/\rho)]$.

We used a 120-μm-long SMR with an internal fluid channel of 3 μm by 5 μm, driven in the second vibrational mode ($f \approx 2.1$ MHz). A schematic of the cantilever with embedded fluid channel is shown in Fig. 1a. The chip containing the SMR is mounted on a fluidic manifold, and computer-controlled pressure regulators with pressurized glass sample vials are used to precisely control fluid flow within the SMR as previously described (31). Spores are suspended in the desired solution, allowed to equilibrate for 30 min, and loaded into the sample bypass channel. Sample fluid is directed through the resonator, and the buoyant mass for individual spores is determined as they flow through the cantilever.

**Centrifugal trapping and spore water exchange.** Bacterial spores can be trapped at the end of the cantilever when centrifugal force (proportional to the vibrational amplitude squared) becomes greater than the force due to fluid flow through the channel (32). To initiate trapping of bacterial spores, the drive amplitude is increased until spores are efficiently trapped at the tip of the resonator at the desired flow rate. Spores are suspended in a solution of sucrose in $H_2O$ at ~25% (wt/vol) (adjusted to match the density of $D_2O$, ~1.1 g/ml) and are loaded into one bypass channel of the SMR chip. The other bypass channel is loaded with pure $D_2O$. The direction of flow through the resonator is reversed, replacing the sample solution from the first bypass channel with $D_2O$ from the
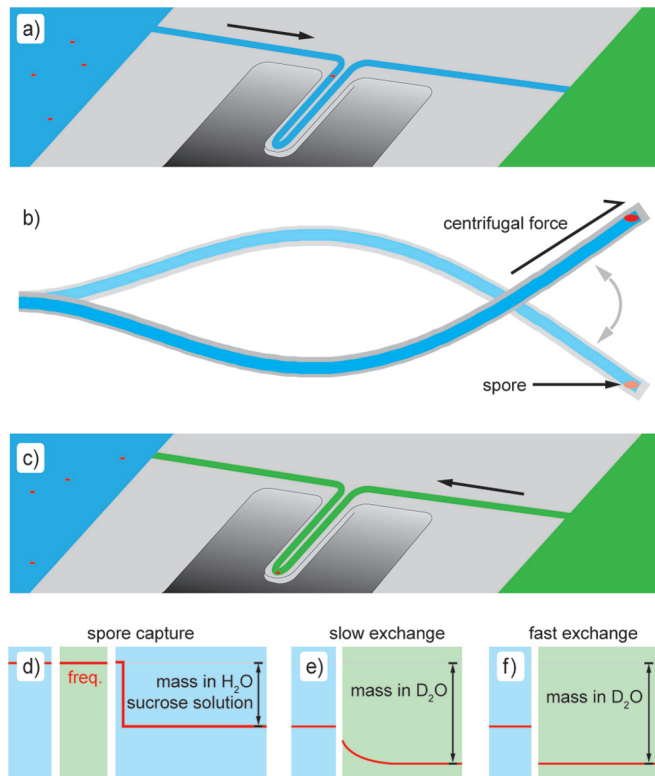
**FIG 1** Measurement schematic. (a) The buoyant mass of individual spores is determined as they pass through a fluid channel embedded in a resonating cantilever. (b) Spores can also be trapped at the end of the cantilever (cross section) by centrifugal force. (c) The fluid within the resonator can be exchanged with the fluid in the other bypass, while the spore remains trapped. The expected mass signal is demonstrated for spore capture (d) and for slow (e) and fast (f) $H_2O$-to-$D_2O$ exchange. freq., frequency.

second. A schematic representation of spore trapping and fluid exchange is shown in Fig. 1a to c. As indicated in Results, some experiments were performed with the exchange between solutions in the reverse of this order. The background signal that results from fluid exchange in an empty resonator is recorded prior to the trapping of any spores. Spores enter the cantilever and are trapped at the tip, where they remain during subsequent exchange from the sample solution to $D_2O$. Spores are exchanged back into the sample solution, from which additional spores enter the trap. Multiple rounds of exchange with successive trapping of spores are performed. The resonator frequency is recorded throughout these exchanges, and the signal due to the buoyant mass of the spores is obtained by subtracting the background signal. The change in buoyant mass is calculated from the difference in baseline frequencies between the two solutions before and after the trapping of spores (Fig. 1d).

## RESULTS

**Buoyant mass.** Buoyant mass quantifies how much a spore weighs in excess of the fluid that it displaces (see Materials and Methods). The buoyant mass of a spore in solutions of two different densities can be used to calculate the mass, volume, and density of the cell. Likewise, measurements in $H_2O$ and $D_2O$ solutions can be used to separately quantify the dry and aqueous contents (31). To determine the distribution across the population, the buoyant mass of ~1,000 individual hydrated *B. subtilis* (PS533; wild-type) spores is determined by weighing them in an SMR. Buoyant mass profiles for spores determined in $H_2O$ ($\rho \approx 1.0$), in 97.5% $D_2O$ ($\rho \approx 1.1$

g/ml), and in $H_2O$ solutions of glycerol, sucrose, and Percoll (colloidal suspension) at ~1.1 g/ml are shown in Fig. 2a. Spores in $H_2O$ have a density of ~1.2 g/cm³ determined by density gradient ultracentrifugation (33) and therefore have a positive buoyant mass because they weigh more than the $H_2O$ that they displace. For these measurements, spores have the greatest buoyant mass in water. The other fluids are all prepared at the same density (1.1 g/ml) and result in a reduced buoyant mass relative to measurements in pure $H_2O$ because the difference between spore density and solution density is lower. The buoyant masses of solid particles in the four solutions at 1.1 g/ml are equivalent because the particles displace an equal volume (and mass) of each fluid (data not shown). However, spores are not solid particles, and the molecules in each solution can permeate the spore to different extents, as shown schematically in Fig. 2b. Molecules that have permeated into the spore add to the buoyant mass determined for each spore as they displace less dense $H_2O$ molecules.

**Physical properties of intact spores.** The size and density of a spore determine its buoyant mass in a given solution. Because these parameters vary from spore to spore, we obtained a distribution of buoyant masses under each condition (Fig. 2a). Several biophysical parameters for the wild-type spore population can be calculated from the buoyant mass distributions shown in Fig. 2a. For example, the median buoyant mass of the spores in $H_2O$ (165 fg; coefficient of variation [CV], 23%) and Percoll (89 fg; CV, 36%) defines a line for which the slope is an estimate of the median spore volume (0.76 μm³). The x-intercept is an estimate of the spore density (assuming all spores are equally dense), which we calculate as 1.22 g/cm³, a value nearly identical to that determined by ultracentrifugation on a Percoll gradient (33). Although the population data collected here cannot directly address variability in single-spore volume and density, if we assume all spores are equally dense, then the volume CV is equal to the buoyant mass CV. The assumption of roughly constant density is likely valid, given previous work showing that variation in cell size is generally far greater than in cell density (34–36). Indeed, dry spore volumes quantified by electron microscopy (35) show a CV of 21%, similar to what we observe for buoyant mass.

As with the measurements in water and in Percoll, we can also compare differences between buoyant mass measurements in $H_2O$ and $D_2O$ to estimate the properties of the dry spore. Because $D_2O$ molecules entirely replace $H_2O$ throughout the spore, only the dry content is responsible for the difference in buoyant mass between these solutions. The line between the buoyant masses in $H_2O$ and $D_2O$ (128 fg; CV, 18%) determines the dry volume to be 0.37 μm³ and the dry density to be 1.45 g/cm³, which is also consistent with previously determined values (33).

The $H_2O$ content of spores can be calculated based on the difference between the total spore content and the dry spore content. If we extrapolated the lines shown in Fig. 2c back to a solution density of 0 g/ml, the y-intercepts (not shown) would represent the median spore's total mass and dry mass. The difference between the two is the mass of the spores' $H_2O$, estimated here to be 390 fg. Alternately, any two points of equivalent density on these lines can be subtracted to find the buoyant mass of the $H_2O$ with respect to the solution density. As shown in Fig. 2c, a spore is 39 fg heavier in $D_2O$ than in Percoll. $H_2O$ is only 0.1 g/ml less dense than $D_2O$ (1.1 g/ml), so to obtain the total $H_2O$ content (density of 1.0 g/ml), the difference between the Percoll and $D_2O$ measurements must be scaled by a factor of 10.
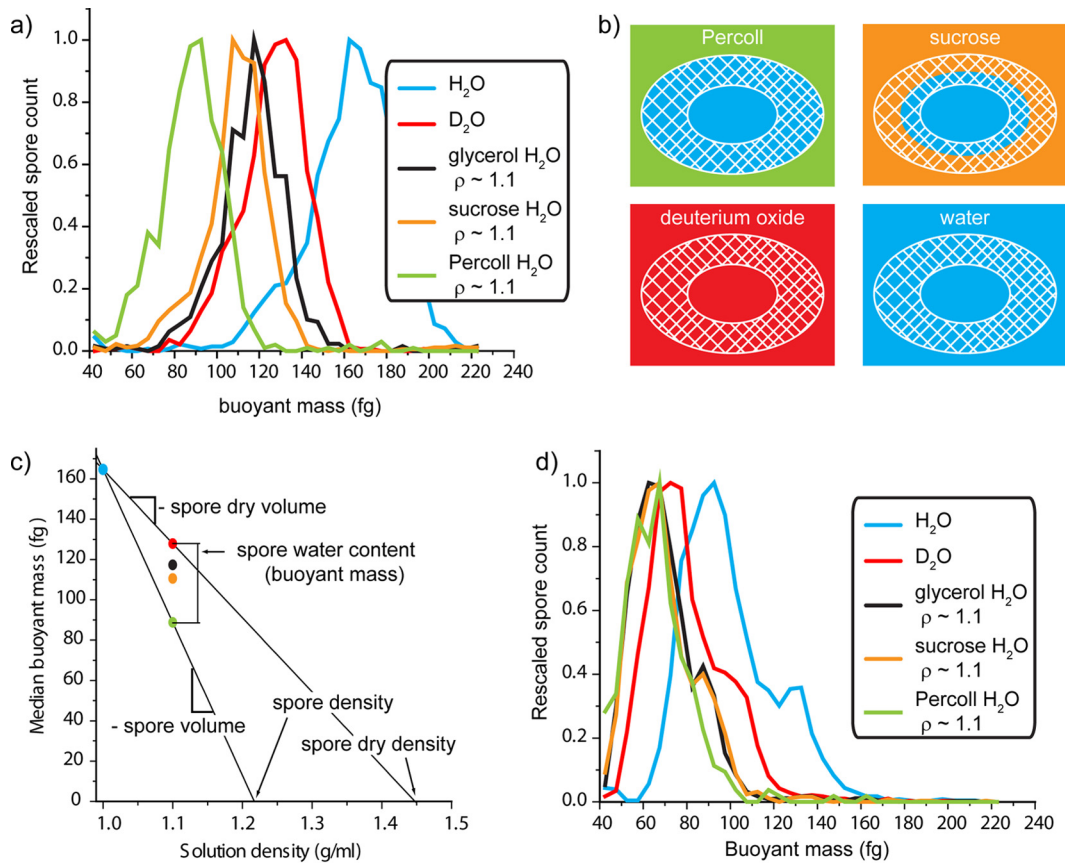
FIG 2 (a) The buoyant mass distributions for individual wild-type spores are shown in various solutions. These molecules permeate the spores to different extents (b), and the resulting differences in buoyant mass can be used to calculate a number of biophysical parameters for the spores (c). (d) The buoyant mass profiles of PS4150 (*cotE gerE* mutant) spores are shown in the same solutions.

**Molecular permeation based on buoyant mass.** The above-described determination of $H_2O$ content represents the extremes of spore permeability. Percoll is a colloidal suspension of 15 to 30 nm polyvinylpyrrolidone-coated silica particles that are expected to be completely excluded from spores, whereas $D_2O$ is not excluded at all and can entirely replace a spore's internal $H_2O$. In between these extremes, small molecules can permeate some portion of solvent space within the spore. The cortex of a spore is accessible to small molecules, such as nutrients that must reach the IM to initiate germination, although it is traditionally difficult to measure the volumes accessible to these molecules. By measuring the buoyant mass of spores in solutions of small molecules of various sizes, we show that it is possible to probe the internal volume of the spore that is accessible to these molecules (Fig. 2b). We have chosen neutral, highly soluble molecules for this assay to minimize the extent to which they interact with the spore. However, we note that chemical interactions or other forces that concentrate molecules within the spore will increase the buoyant mass of the spores. Similarly, repulsion or exclusion of these molecules would decrease the buoyant mass of spores. The median buoyant masses of wild-type spores in the sucrose and glycerol solutions are 111 fg (CV, 19%) and 117 fg (CV, 21%), respectively. Compared to the Percoll measurement, we observe that an additional buoyant mass of 22 fg sucrose and 28 fg glycerol can permeate the outer layers of the spore at these concentrations. Assuming a uniform distribution of these molecules, the additional mass in glycerol relative to sucrose indicates that there is a greater volume within the cortex that is accessible to glycerol, and this is consistent with previous work on the levels to which different molecules can permeate the spore (4). If we assume that these solutes diffuse into the spore's interior volume to the same concentration as that outside the spore, these values suggest that of the 0.39 $\mu m^3$ occupied by water, 0.22 $\mu m^3$ is accessible to sucrose and 0.28 $\mu m^3$ is accessible to glycerol.

**Physical properties and permeation in coat-defective spores.** Due to the fact that they lack most coat layers (37), spores with mutations in both *cotE* and *gerE* genes have been characterized in the literature by a number of different techniques. Relevant to the studies here, the near-total lack of a coat has been directly visualized by atomic force microscopy (AFM) (37), and they have been found to have significantly more rapid core water permeability than wild-type spores (22). The buoyant masses of *cotE gerE* spores were determined for the solutions described above (Fig. 2d). Overall, the buoyant masses for these spores are lower than for wild-type spores. Because a number of the genes regulated by GerE are not specific to the assembly of the coat (38), it is likely that some of the mass difference is due to loss of specific proteins or structures besides just the coat. Nevertheless, the loss of coat biomaterial (and hence buoyant mass) is consistent with observations from AFM that these spores are almost entirely devoid of a

coat (37). There, it was noted that some spores still retain patches of coat material. We note that there appear to be two peaks in the buoyant mass distribution for *cotE gerE* spores. For example, in the blue line in Fig. 2d, where the spores' buoyant masses were determined in $H_2O$, the population has a median buoyant mass of 95 fg (CV, 26%); however, the left-hand portion of this distribution appears to be a primary population with a lower buoyant mass centered at ~90 fg and a less abundant subpopulation centered at ~130 fg, which we suspect are spores that retain a portion of their coat.

The permeability to molecules in *cotE gerE* spores is also very different from that of wild-type spores. The median buoyant masses of these spores in glycerol and sucrose are identical (67 fg; CV, 27%), suggesting that these two molecules enter the spore to the same extent. Unlike intact spores, spores with severely damaged coats cannot exclude larger molecules from the peptidoglycan cortex; hence, many coat mutants become lysozyme sensitive (11). The median buoyant mass is 65 fg (CV, 23%) in Percoll, which consists of colloidal silica particles that are large relative to glycerol and sucrose molecules. The fact that sucrose and glycerol increase the buoyant mass to the same degree as each other and only slightly more than Percoll suggests that the cortex is not providing a differential barrier to these different-sized molecules in *cotE gerE* spores as it does in wild-type spores. This suggests that the cortex of coat-damaged spores has open volumes that are much more accessible to external solvent than in intact spores. As noted above, some changes in cortex structure may exist in this mutant beyond those caused by the lack of a coat, due to the variety of genes regulated by GerE (38). Interestingly, the shape of the buoyant mass distribution for these spores is different in Percoll from the shape in other solutions, and the heavier subpopulation is no longer apparent. If this population were to exclude Percoll from some interior volume, the space would remain filled with only $H_2O$, and the spore would weigh less than if the volume were filled with a heavier solution.

To calculate the $H_2O$ content of *cotE gerE* spores, we subtract the median buoyant mass in Percoll (65 fg; CV, 23%) from that in $D_2O$ (76 fg; CV, 26%), yielding an $H_2O$ buoyant mass of 11 fg. Note that an 11-fg buoyant mass from $H_2O$ when weighed in a solution density of 1.1 g/ml is equivalent to a total $H_2O$ mass of 110 fg. Glycerol (the smallest of the permeating molecules) is expected to approach the IM to an extent similar to that of $H_2O$. If this is true, the 9-fg buoyant mass of $H_2O$ (total mass, 90 fg) that glycerol cannot replace represents mostly core $H_2O$.

**Kinetics of buoyant mass change.** The buoyant mass measurements for Fig. 2 are useful for measuring the characteristics of a population at equilibrium or undergoing slow changes (on the order of minutes or more), but water permeation of spores occurs on a time scale of seconds or less. To study spore water permeation on a subsecond time scale, we developed a technique to trap spores at the tip of the cantilever and monitor the spore's buoyant mass during the transition between two fluids, as shown schematically in Fig. 1. For a typical assay, spores are initially suspended in a sucrose solution at ~1.1 g/ml and are exchanged into pure $D_2O$. The change in buoyant mass that occurs for PS533 (wild-type) spores is shown in Fig. 3a. Data are aligned such that time point zero ($t = 0$) is the time when the fluid exchange in an empty resonator is complete. Curves of increasing magnitude are the result of successively trapping multiple spores, annotated to the right of the curves, and repeating the fluid exchange. The y axis for

these plots represents the change in buoyant mass of the spores between the two solutions and is determined from the difference between the mass signals—SMR resonant frequency—in each fluid, as shown in Fig. 1d and e.

Exchanging spores from a sucrose–$H_2O$ solution to $D_2O$ results in the movement of all three of these species within different parts of the spore. In Fig. 3a, we observe an increase in mass consistent with the replacement of $H_2O$ with $D_2O$. We also expect the sucrose molecules from the initial solution to diffuse out of the spores, but we do not observe a loss in mass over the several seconds following the fluidic exchanges. This suggests that either the sucrose leaves the spores concurrently with (or more quickly than) replacement by $D_2O$ or the sucrose leaves over a time scale that is longer than a few seconds, illustrated schematically in Fig. 3b. The buoyant mass obtained from the spore populations (Fig. 2) can be used to inform our interpretation of the kinetic data. Population data are acquired over a much longer time period (30 to 60 min) and can be considered endpoints for the exchange kinetics. According to the median population values reported above, we expect each spore to gain ~39 fg buoyant mass due to uptake of $D_2O$ and to lose ~22 fg buoyant mass of sucrose, a net increase of ~17 fg.

To determine if the kinetic measurements are consistent with the endpoint population measurements, we repeatedly measured the buoyant mass of spores ~9 s after a fluid switch from sucrose in $H_2O$ to $D_2O$ and normalized to the number of spores that were trapped in the resonator at the time (Fig. 3c). To account for experimental variation outside calculated error bars (see the supplemental material), values and standard errors reported here are determined from replicate fluid switches in which at least 10 spores were trapped in the resonator. The per-spore mass change after ~9 s in $D_2O$ was 17.9 ± 0.6 fg (mean ± standard error [SE]). Similarly, an exchange in which the spores were switched into $D_2O$ for 1 min prior to the buoyant mass determination (green dots in Fig. 3c) yielded a value of 17.7 ± 0.8 fg. The close agreement between these values and the estimate of the population endpoint (17 fg) shows that the bulk of the sucrose leaves the spore either faster than or concurrent with the exchange of $H_2O$ for $D_2O$. However, a careful error analysis reveals that it is still possible for a buoyant mass of up to 1.7 fg of sucrose to remain within the spore and not be detected by our method (see the supplemental material).

**Water permeability of coat mutant spores.** Previous analysis by nuclear magnetic resonance (NMR) has shown that *cotE gerE* mutant spores have a greatly increased water permeability (22). Figure 3d shows the result of our fluid exchange analysis on these spores. Unlike the wild-type spores shown in Fig. 3a, fluid exchange with *cotE gerE* spores appears to already be complete by the time the resonator is fully flushed (~200 ms) (Fig. 3d), which is consistent with the previous report using NMR. CotE is a protein required for normal coat assembly, and *cotE* spores lack a number of coat proteins and appear to lack an outer coat (5). GerE is a transcription factor that regulates a number of proteins, many of which are involved in assembly of the coat, but also many others of which control disparate processes during spore formation (38). Thus, while these spores are severely coat defective, there may be other aspects of this mutant that affect its water permeability.

In order to address the importance of the coat to spore water permeability, we have characterized water exchange for spores with a number of additional mutations that are known to affect
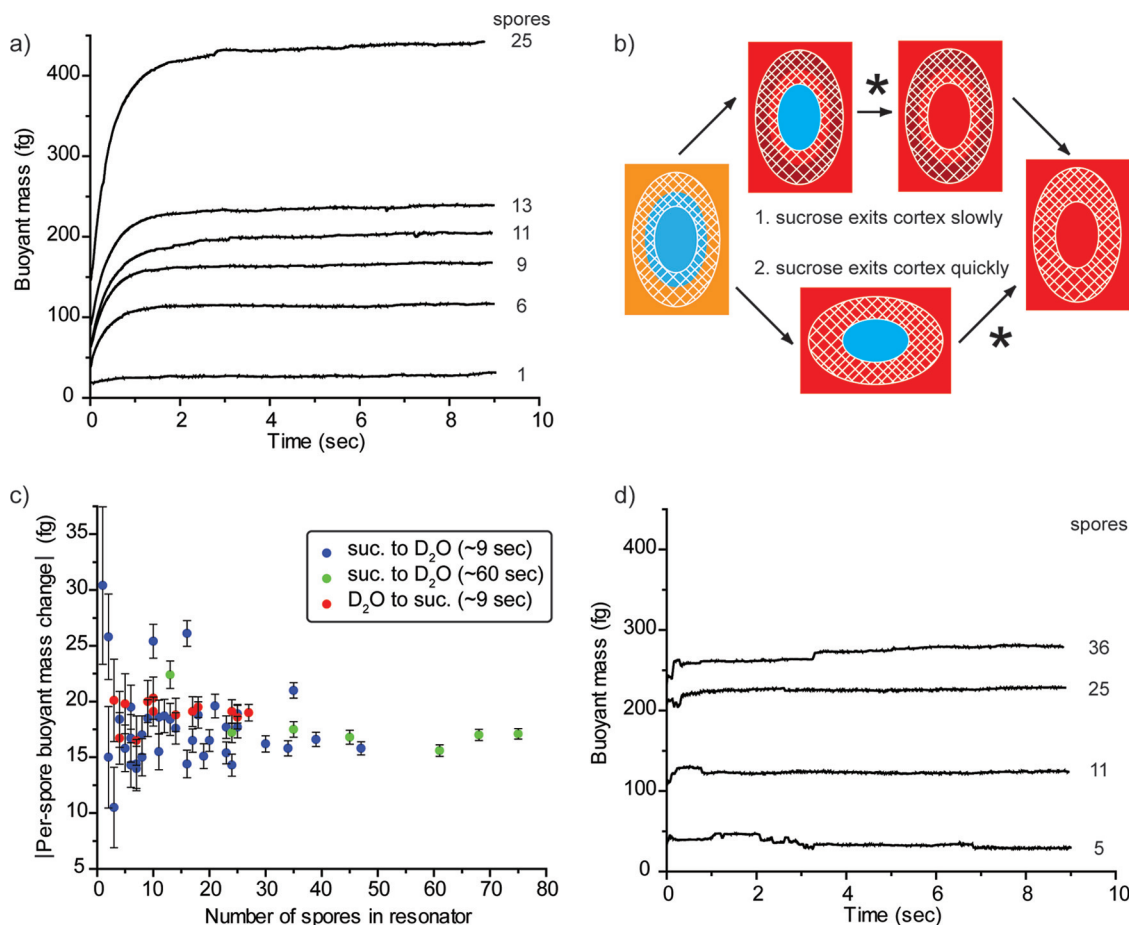
FIG 3 The buoyant mass of spores trapped at the tip of the cantilever is observed immediately after the resonator is exchanged from an H$_2$O-sucrose (25%) solution to pure D$_2$O. (a) Wild-type spores show a slow increase in buoyant mass from the replacement of internal H$_2$O with D$_2$O. (b) Sucrose leaving the spore is noted with an asterisk in alternate scenarios, either after replacement of internal H$_2$O with D$_2$O or before this exchange occurs. (c) These scenarios can be evaluated by quantifying the total change in buoyant mass per spore for reactions that occur over different time scales and in the reverse order. For example, data from panel a and replicate experiments are shown in blue. The experimental variation observed here is greater than the calculated error bars because spores do not remain in exactly the same position, as the direction of fluid flow is switched back and forth and the SMR's frequency is highly dependent on the position of mass within the resonator. Similarly, irregularities are seen in the kinetic traces of some experiments as spores shift position. (d) The buoyant mass change for *cotE gerE* mutant spores takes place on a time scale that is less than the temporal resolution of the measurement.

coat formation (Fig. 4). Kinetic traces for mutants not shown above (Fig. 3) are presented in Fig. S2 in the supplemental material, and time constants determined for all spores are shown in Fig. 4. The time constants determined for these exchange reactions suggest that all coat mutations studied here affect the permeability of the resulting spore at some level. On the extreme end, several coat mutations appear to completely abrogate the relatively slow exchange seen with the wild-type spores. The *gerE* and *safA* mutations (alone or in conjunction with mutation in *cotE*) result in spores whose H$_2$O appears to have been nearly completely exchanged within the time required to fully flush the cantilever with D$_2$O, as does the *spoVID* mutation. We estimate 0.09 s as an upper bound on the time constant for these spores.

The *cotE* mutation results in spores for which most of the H$_2$O has exchanged by time zero (*t* = 0), although there is some observable exchange. It is interesting that significant heterogeneity in coat structure has been observed by AFM of *cotE* spores (37). It may be that this mutation results in spores with differential permeability to water as well, with less permeable spores contributing

to the amplitude of the observed exchange and quickly exchanging spores only contributing to the overall amplitude of the curves. Indeed, for *cotE* spores, 80% of the H$_2$O is exchanged within the time required to flush the channel, while for the *cotH* and *cotXYZ* mutants, whose exchange rates are equivalent to the *cotE* mutant, this value is ~50% (see Fig. S2 in the supplemental material). The H$_2$O exchange for *cotO* and *cotB* mutant spores is increasingly slow, suggesting that these mutations have a less deleterious effect on spore water permeability. Interestingly, a *cotXYZ* mutation, which results in the loss of spores' outermost crust layer, also resulted in increasing spore water permeability to a level similar to that of *cotH* mutant spores (Fig. 4).

**Molecular permeation based on spore germination.** The results described above indicated that coat defects have significant effects on permeation of molecules, including water, into spores. To examine if this is also the case for other small molecules that are thought to exert their effects by acting at a spore's inner membrane just outside the spore's core, we examined spores' permeation by two compounds, Tb$^{3+}$ and dodecylamine, that can influ-
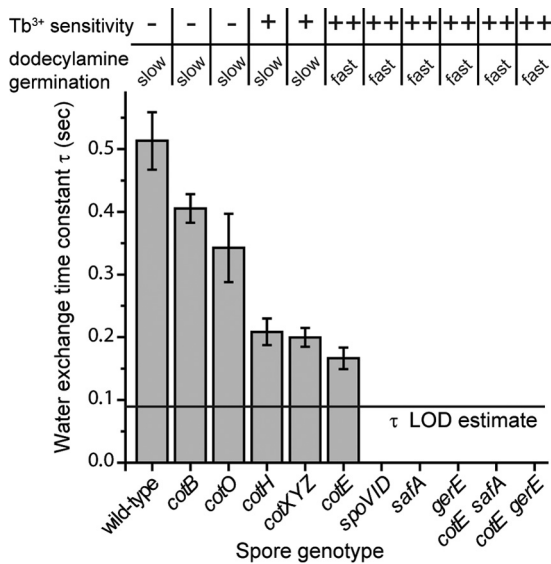
FIG 4 The time constants for $H_2O$-to-$D_2O$ exchange are determined by fitting the kinetic traces shown in Fig. 3a and d and in Fig. S2 in the supplemental material to an exponential decay equation, $y = a + b(1 - e^{-t/\tau})$. Under the flow conditions used for these experiments, it takes ~200 ms to completely replace the fluid in the embedded channel. Time constants were not determined for spores in which the exchange appears to be complete by this time. Rather, we estimate an upper bound as our limit of detection (LOD), here assumed to be 0.09 s (yielding an exchange that is 90% complete after 200 ms), indicated by a horizontal line on the plot above. The results for $Tb^{3+}$ sensitivity of L-valine germination and rates of dodecylamine germination (slow germination is <50% of the rate of fast germination) are taken from data in Fig. 5 and data not shown. −, minimal inhibition; +, intermediate inhibition; ++, nearly complete inhibition.

ence spores' return to life in the process of germination (27, 29, 34). TbCl₃ at ~50 μM is often used to monitor the progress of spore germination, by measuring DPA release via Tb-DPA complex formation (28). TbCl₃ at 50 μM only minimally inhibits the germination of intact spores but completely inhibits the germination of severely coat-defective spores (29). The mechanism for this inhibition has not been definitively established, but it has been suggested that $Tb^{3+}$ binds to DPA being released from the protein channel in spores' IM through which DPA is released and the Tb-DPA complex blocks this channel completely. If this is the case, then $Tb^{3+}$ needs to penetrate to the IM to inhibit spore germination, something that should be much easier in coat-defective spores. To test the effects of TbCl₃ on the germination of the wild-type and various coat mutant *B. subtilis* spores used to measure water permeation, we monitored the germination of these spores with the nutrient germinant L-valine with $Tb^{3+}$ either present throughout the germination process or only added at various times (Fig. 5a, c, and e and data not shown). Notably, spores of all severely coat-defective strains (i.e., those that produce lysozyme-sensitive spores [11]; with mutations in *safA*, *spoVID*, *cotE*, *gerE*, *cotE gerE*, and *cotE safA*) exhibited complete or almost complete lack of germination in the continuous presence of TbCl₃, although these spores germinated reasonably well in the absence of $Tb^{3+}$. The *cotH* and *cotXYZ* spores exhibited less significant inhibition of spore germination by TbCl₃, with spores of other coat-defective strains exhibiting only minimal inhibition (Fig. 4 and 5). The sensitivity of spore mutants to inhibition of germination by $Tb^{3+}$

appears to be correlated with the water permeability of the core (Fig. 4).

While spores normally germinate with nutrient germinants such as L-valine, they also germinate with some nonnutrient germinants, such as cationic surfactants like dodecylamine (27). This molecule most likely triggers germination by directly opening spores' IM channel for DPA, probably by binding to SpoVAC, one of the seven IM SpoVA proteins that likely comprise this channel (27, 39, 40). In order to bind to SpoVAC, the dodecylamine must penetrate through spores' outer layers to access the IM, and it is certainly possible that rates of spore germination with dodecylamine are dependent on the rate of permeation of this agent through spores' outer layers. Indeed, chemical decoating and at least one severe coat defect increase rates of dodecylamine germination of *B. subtilis* spore germination markedly (27). Examination of the rates of dodecylamine germination of the wild-type and coat mutant spores with TbCl₃ added at various times in germination gave results that were concordant with those seen with effects of TbCl₃ on L-valine germination (Fig. 5b, d, and f and data not shown). Thus, the more severely coat-defective spores (with mutations in *safA*, *spoVID*, *cotE*, *gerE*, *cotE gerE*, and *cotE safA*) had much higher rates of dodecylamine germination than wild-type or *cotO*, *cotB*, *cotH*, or *cotXYZ* mutant spores. The germination of mutant spores with dodecylamine also appears to correlate with the water permeability of the spore core (Fig. 4).

## DISCUSSION

We report here a method for observing the water and small-molecule permeability of bacterial spores based on the buoyant mass of these particles in different solutions and on the increase in mass that occurs when internal $H_2O$ is replaced by $D_2O$. While it was once hypothesized that water in the core of *B. subtilis* spores was essentially immobile, it has been demonstrated that spore core water is (i) mobile and (ii) free to exchange with external water, albeit at a rate that is significantly lower than that for vegetative cells (4, 17, 20, 22). It has generally been regarded that permeability of the inner membrane that surrounds the core is the primary barrier to exchange with external water.

The IM of coat-defective spores has permeability to methylamine and lipid mobility similar to that of wild-type spores (12–15). However, we find that the rate at which core water is exchanged is altered significantly for a number of coat mutants, with several mutations that exchange faster than the ~200-ms temporal resolution of our assay. Similarly, measurements of water ²H relaxation rates by NMR spectroscopy indicate that the water permeability of the *B. subtilis* spore IM is ~25-fold greater in *cotE gerE* spores than in wild-type spores (22), and decoating spores also increases rates of ¹²⁹Xe movement into the spore core (21). Two possible explanations for this apparent discrepancy are as follows. (i) The IM is the barrier to exchange of core water in wild-type spores, but that barrier becomes defective in damaged spores. If this is the case, then the permeability of the IM may require the integrity of spores' outer layers, which affect IM structure in a way that alters its permeability to water but not to methylamine. (ii) The IM is not the barrier to water entering the spore core, in which case some structure outside the IM must provide this barrier.

Here we investigate the role of the spore coat in maintaining the low water permeability of the core. We find that spores lacking CotB, a major component of the outer coat, have permeability similar to that of the wild-type spores. Spores lacking CotO or
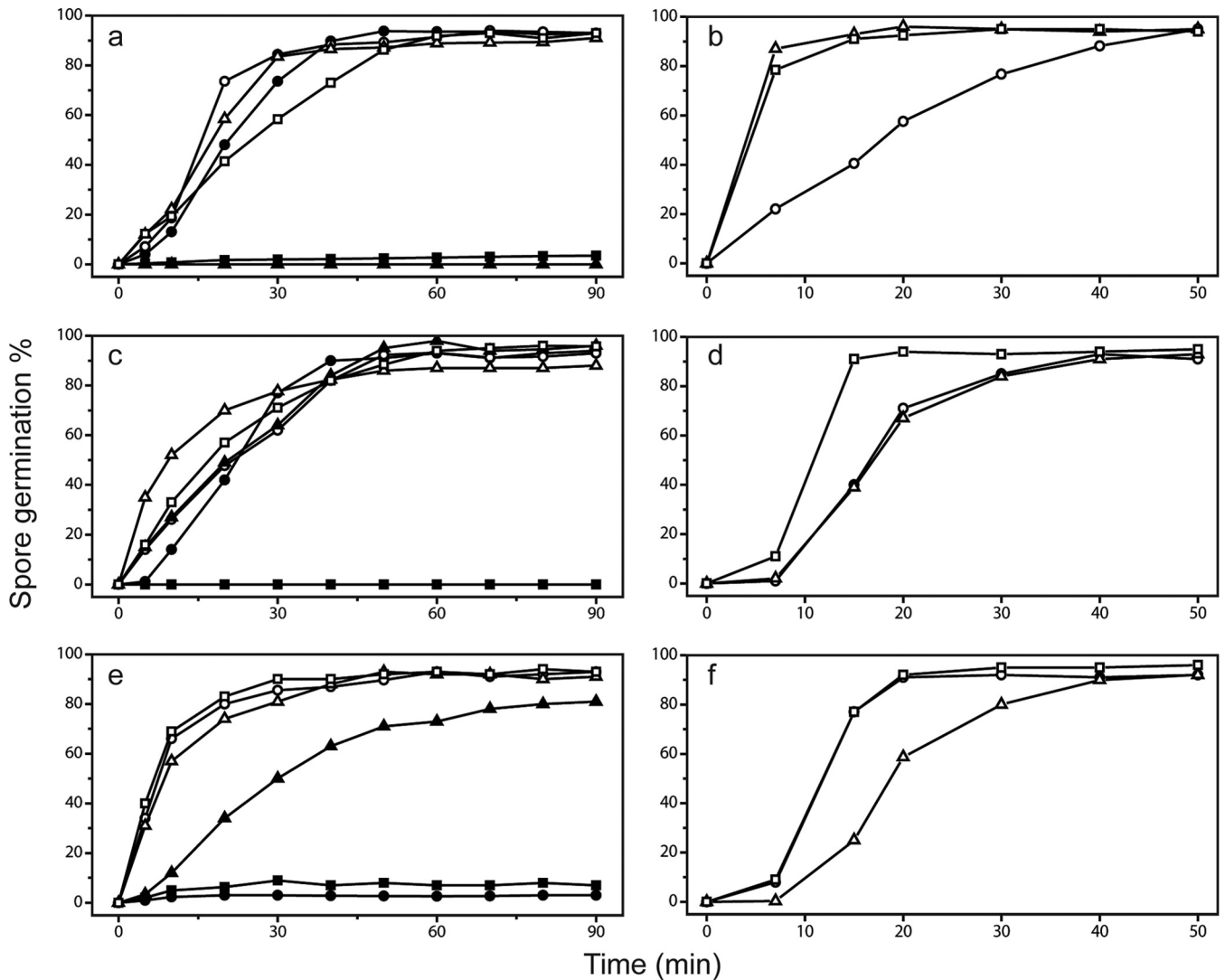
FIG 5 (a to f) L-Valine and dodecylamine germination of spores of wild-type and coat mutant *B. subtilis* spores. Spores of various strains were germinated with either L-valine (a, c, e) or dodecylamine (b, d, f) with TbCl₃ present either from the beginning of germination (●, ▲, and ■) or added at various times (○, △, and □) as described in Materials and Methods. The symbols denoting the spores analyzed in the various panels are as follows. For panels a and b: ○ and ●, PS533 (wt); △ and ▲, PS4150 (*cotE gerE* mutant); □ and ■, PS3328 (*cotE* mutant). For panels c and d, ○ and ●, PS4133 (*cotB* mutant); △ and ▲, PS4134 (*cotO* mutant); □ and ■, PS4149 (*gerE* mutant). For panels e and f, ○ and ●, PS3735 (*spoVID* mutant); △ and ▲, PS3736 (*cotH* mutant); □ and ■, PS3738 (*safA* mutant).

CotH, which control the assembly of a number of outer coat proteins, display more-significant increases in the rate of water exchange. Similarly, loss of CotE, which localizes to a layer between the inner and outer coats and guides outer coat formation, results in even faster exchange. Although this trend suggests that proteins residing between the outside of the spore and the inner coat have increasing effects on the rate of water exchange, *cotXYZ* spores, which lack the outermost crust layer, display an exchange rate equivalent to that of *cotE* spores. Consistent with this result, it has been suggested that the spore crust may contribute to the structure of the outer coat, as this layer is easily disrupted in spores lacking CotXYZ (41). All of the other mutations tested exchange water faster than the current limit of detection of this assay. Of these, SpoVID and SafA are both involved early in coat formation and GerE is a transcription factor that regulates many proteins involved in coat formation, as well as other processes (38). Double

coat mutant spores, which have increased loss of coat material, also exchange faster than the limit of this assay.

The coat itself likely cannot be a barrier to water, as it does not provide a barrier to molecules that are much larger. For instance, it has long been known that small molecules can permeate the coat and beyond (4), and dyes used to determine the surface area of spores confirm this porous nature (42). However, we find that removing or compromising the coat removes the barrier to core water permeability. One possibility is that upon exiting the core, water interacts specifically with outer layers of the spore in a way that small molecules cannot. The cortex of the spore is hygroscopic, and mechanical changes occurring on the same time scale as those observed herein have been observed for spores upon changes in relative humidity (43). However, these changes still occur in *cotE gerE* spores, whereas these mutations abolish the low water permeability in this work and as observed by NMR. If the

mechanism connecting these disparate spore regions involves the intermediate layers, in particular the cortex, either by the creation of an alternate barrier or by modulation of an existing barrier (the IM), measuring the molecular and water permeability of spore cortex or other mutants could provide additional insights. For example, we may find mutations that change the structure of the cortex or of the inner membrane in a way that abolishes this barrier even in the presence of an intact coat.

The data presented here also show a correlation between the rate at which spores exchange $H_2O$ with external $D_2O$ and the ability of both $Tb^{+3}$ and dodecylamine to gain access to the IM, as measured by a germination assay. In addition, wild-type spores are shown to allow a greater extent of permeation to small molecules than to larger ones, a characteristic that is abolished in coat-defective spores. Taken together, these results support the notion that molecular access to the IM (the rate at which molecules are able to get up to the IM) may limit the rate at which molecules are able to cross the IM, even for molecules as small as water.

The space that appears to be freely solvent accessible within a *B. subtilis* spore is in the coat and the peptidoglycan cortex (4, 17, 44). In a simple biophysical model of the spore, we might envision the cortex as a series of water- and small-molecule-accessible spaces of decreasing size as one approaches the core. We would expect that the larger, outer accessible areas are essentially open space relative to the size of molecules but at some point become restrictive on this scale. That is, solvent-accessible space within the cortex may simply keep decreasing as one approaches the core to the extent that there are simply very few places through which water and other molecules can pass to access the inner membrane. This model is consistent with our observation that glycerol (92.1 Da) can invade the spore to a greater extent than sucrose (342.2 Da), as was also observed by bulk solute uptake measurements for molecules differing by 4 orders of magnitude in molecular weight (4).

The bulk of cortex space is indeed freely accessible, as we find that the majority of the sucrose leaves the spore on a time scale that is either comparable to or faster than the $H_2O$-$D_2O$ exchange. Under the model proposed above, we might expect that some small molecules that have been taken up by the spore into areas that are restrictive to their permeation could be observed leaving the spore at a lower rate during the fluid exchange assays. However, while some sucrose may remain in the spore after exchange of water, its loss was not directly observed. Finally, a mechanism to form a gradient of solvent-accessible space is not known. This could possibly be achieved by changes in molecular packing or in changes in the structure of the cortex itself. It has been observed that cortex cross-linking appears to be highest at the outer part of the cortex, with 2- to 8-fold-lower cross-linking just outside the germ cell wall adjacent to the IM (45, 46), although it is not clear how cross-linking would affect solvent-accessible space. Subsequent work may elucidate characteristics of the spore that affect their permeability to water and small molecules. Molecular exclusion within the cortex has been demonstrated across a wide range of molecule sizes for *Bacillus cereus* (4), and we show here that while similar permeability differences for *B. subtilis* wild-type spores exist, this difference is abolished in severely coat-defective spores. It will be interesting to determine the extent to which these permeability differences exist in spores with only minor coat defects, and if so, whether they show any correlation with the observed loss of a barrier to water permeability.

The SMR provides a direct way to track the motion of molecules into and out of the spore based on the addition or loss of mass, and the use of $D_2O$ enables us to look at the motion of $H_2O$ in addition to dissolved molecules. Similarly, nuclear magnetic resonance (NMR) experiments and Raman spectroscopy have also used $D_2O$ to investigate spore water. The main benchmarks by which we can compare these are the sample size and time scale of the experiments. Raman spectroscopy also has been used to investigate individual spores; however, the temporal resolution of this technique is currently limited to $\sim$2 data points per second (20). NMR experiments can be performed across a wider range of time scales but are typically made on bulk samples consisting of grams of spores, with additional purity considerations like the need to eliminate manganese ions from spore preparations.

The SMR is a microfluidic device capable of using very small sample volumes. For population measurements, we typically assay $\sim$1,000 individual spores, and kinetic data are available down to the individual spore level, although we typically acquire these data with up to $\sim$20 to 30 spores. The temporal resolution of our kinetic measurements is $\sim$10 ms and is limited by the stability of the resonator system (see Fig. S1 in the supplemental material). For our population measurements, the temporal resolution is limited by the time required to measure a statistically representative number of spores (typically less than 1 hour). Population measurements may ultimately prove useful for enabling transport properties to be measured over long time scales (hours to days).

## ACKNOWLEDGMENTS

## FUNDING INFORMATION

## REFERENCES

1. **Setlow P, Johnson EA.** 2013. Spores and their significance, p 45–79. *In* Doyle MP, Buchanan R (ed), Food microbiology, fundamentals and frontiers, 4th ed. ASM Press, Washington, DC.
2. **Cortezzo DE, Setlow P.** 2005. Analysis of factors that influence the sensitivity of spores of *Bacillus subtilis* to DNA damaging chemicals. J Appl Microbiol **98:**606–617. http://dx.doi.org/10.1111/j.1365-2672.2004.02495.x.
3. **Driks A.** 1999. *Bacillus subtilis* spore coat. Microbiol Mol Biol Rev **63:**1–20.
4. **Gerhardt P, Black SH.** 1961. Permeability of bacterial spores. II. Molecular variables affecting solute permeation. J Bacteriol **82:**750–760.
5. **Henriques AO, Moran CP.** 2007. Structure, assembly, and function of the spore surface layers. Annu Rev Microbiol **61:**555–588. http://dx.doi.org/10.1146/annurev.micro.61.080706.093224.
6. **Setlow P.** 2006. Spores of *Bacillus subtilis*: their resistance to and killing by radiation, heat and chemicals. J Appl Microbiol **101:**514–525. http://dx.doi.org/10.1111/j.1365-2672.2005.02736.x.
7. **Setlow P.** 2013. Resistance of bacterial spores to chemical agents, p 121–130. *In* Fraise AP, Maillard J-Y, Sattar SA (ed), Principles and practice of

disinfection, preservation and sterilization, 5th ed. Wiley-Blackwell, Oxford, United Kingdom.

8. **Gerhardt P.** 1967. Cytology of *Bacillus anthracis*. Fed Proc **26:**1504–1517.

9. **Koshikawa T, Beaman TC, Pankratz HS, Nakashio S, Corner TR, Gerhardt P.** 1984. Resistance, germination, and permeability correlates of *Bacillus megaterium* spores successively divested of integument layers. J Bacteriol **159:**624–632.

10. **Rode LJ, Lewis CW, Foster JW.** 1962. Electron microscopy of spores of *Bacillus megaterium* with special reference to the effects of fixation and thin sectioning. J Cell Biol **13:**423–435. http://dx.doi.org/10.1083/jcb.13.3.423.

11. **Klobutcher LA, Ragkousi K, Setlow P.** 2006. The *Bacillus subtilis* spore coat provides "eat resistance" during phagocytic predation by the protozoan *Tetrahymena thermophila*. Proc Natl Acad Sci U S A **103:**165–170. http://dx.doi.org/10.1073/pnas.0507121102.

12. **Cowan AE, Olivastro EM, Koppel DE, Loshon CA, Setlow B, Setlow P.** 2004. Lipids in the inner membrane of dormant spores of *Bacillus* species are largely immobile. Proc Natl Acad Sci U S A **101:**7733–7738. http://dx.doi.org/10.1073/pnas.0306859101.

13. **Griffiths KK, Setlow P.** 2009. Effects of modification of membrane lipid composition on *Bacillus subtilis* sporulation and spore properties. J Appl Microbiol **106:**2064–2078. http://dx.doi.org/10.1111/j.1365-2672.2009.04176.x.

14. **Setlow B, Setlow P.** 1980. Measurements of the pH within dormant and germinated bacterial spores. Proc Natl Acad Sci U S A **77:**2474–2476. http://dx.doi.org/10.1073/pnas.77.5.2474.

15. **Swerdlow BM, Setlow B, Setlow P.** 1981. Levels of $H^+$ and other monovalent cations in dormant and germinating spores of *Bacillus megaterium*. J Bacteriol **148:**20–29.

16. **Cortezzo DE, Koziol-Dube K, Setlow B, Setlow P.** 2004. Treatment with oxidizing agents damages the inner membrane of spores of *Bacillus subtilis* and sensitizes spores to subsequent stress. J Appl Microbiol **97:**838–852. http://dx.doi.org/10.1111/j.1365-2672.2004.02370.x.

17. **Gerhardt P, Marquis RE.** 1989. Spore thermoresistance mechanisms, p 43–63. *In* Smith I, Slepecky RA, Setlow P (ed), Regulation of procaryotic development: structural and functional analysis of bacterial sporulation and germination. American Society for Microbiology, Washington, DC.

18. **Kaieda S, Setlow B, Setlow P, Halle B.** 2013. Mobility of core water in *Bacillus subtilis* spores by $^2$H NMR. Biophys J **105:**2016–2023. http://dx.doi.org/10.1016/j.bpj.2013.09.022.

19. **Ghosal S, Leighton TJ, Wheeler KE, Hutcheon ID, Weber PK.** 2010. Spatially resolved characterization of water and ion incorporation in *Bacillus* spores. Appl Environ Microbiol **76:**3275–3282. http://dx.doi.org/10.1128/AEM.02485-09.

20. **Kong L, Setlow P, Li YQ.** 2013. Direct analysis of water content and movement in single dormant bacterial spores using confocal Raman microspectroscopy and Raman imaging. Anal Chem **85:**7094–7101. http://dx.doi.org/10.1021/ac400516p.

21. **Liu G, Bettegowda C, Qiao Y, Staedtke V, Chan KW, Bai R, Li Y, Riggins GJ, Kinzler KW, Bulte JW, McMahon MT, Gilad AA, Vogelstein B, Zhou S, van Zijl PC.** 2013. Noninvasive imaging of infection after treatment with tumor-homing bacteria using Chemical Exchange Saturation Transfer (CEST) MRI. Magn Reson Med **70:**1690–1698. http://dx.doi.org/10.1002/mrm.24955.

22. **Sunde EP, Setlow P, Hederstedt L, Halle B.** 2009. The physical state of water in bacterial spores. Proc Natl Acad Sci U S A **106:**19334–19339. http://dx.doi.org/10.1073/pnas.0908712106.

23. **Westphal AJ, Price PB, Leighton TJ, Wheeler KE.** 2003. Kinetics of size changes of individual *Bacillus thuringiensis* spores in response to changes in relative humidity. Proc Natl Acad Sci U S A **100:**3461–3466. http://dx.doi.org/10.1073/pnas.232710999.

24. **Setlow B, Setlow P.** 1996. Role of DNA repair in *Bacillus subtilis* spore resistance. J Bacteriol **178:**3486–3495.

25. **Nicholson W, Setlow P.** 1990 Sporulation, germination and outgrowth, p 391–450. *In* Harwood C, Cutting S (ed), Molecular biological methods for *Bacillus*. John Wiley and Sons, Chichester, United Kingdom.

26. **Paidhungat M, Setlow B, Driks A, Setlow P.** 2000. Characterization of spores of *Bacillus subtilis* which lack dipicolinic acid. J Bacteriol **182:**5505–5512. http://dx.doi.org/10.1128/JB.182.19.5505-5512.2000.

27. **Setlow B, Cowan AE, Setlow P.** 2003. Germination of spores of *Bacillus subtilis* with dodecylamine. J Appl Microbiol **95:**637–648. http://dx.doi.org/10.1046/j.1365-2672.2003.02015.x.

28. **Yi X, Setlow P.** 2010. Studies of the commitment step in the germination of spores of *Bacillus* species. J Bacteriol **192:**3424–3433. http://dx.doi.org/10.1128/JB.00326-10.

29. **Yi X, Bond C, Sarker MR, Setlow P.** 2011. Efficient inhibition of germination of coat-deficient bacterial spores by multivalent metal cations, including terbium ($Tb^{3+}$). Appl Environ Microbiol **77:**5536–5539. http://dx.doi.org/10.1128/AEM.00577-11.

30. **Burg TP, Godin M, Knudsen SM, Shen W, Carlson G, Foster JS, Babcock K, Manalis SR.** 2007. Weighing of biomolecules, single cells and single nanoparticles in fluid. Nature **446:**1066–1069. http://dx.doi.org/10.1038/nature05741.

31. **Feijó Delgado F, Cermak N, Hecht VC, Son S, Li Y, Knudsen SM, Olcum S, Higgins JM, Chen J, Grover WH, Manalis SR.** 2013. Intracellular water exchange for measuring the dry mass, water mass and changes in chemical composition of living cells. PLoS One **8:**e67590. http://dx.doi.org/10.1371/journal.pone.0067590.

32. **Lee J, Shen W, Payer K, Burg TP, Manalis SR.** 2010. Toward attogram mass measurements in solution with suspended nanochannel resonators. Nano Lett **10:**2537–2542. http://dx.doi.org/10.1021/nl101107u.

33. **Tisa LS, Koshikawa T, Gerhardt P.** 1982. Wet and dry bacterial spore densities determined by buoyant sedimentation. Appl Environ Microbiol **43:**1307–1310.

34. **Grover WH, Bryan AK, Diez-Silva M, Suresh S, Higgins JM, Manalis SR.** 2011. Measuring single-cell density. Proc Natl Acad Sci U S A **108:**10992–10996. http://dx.doi.org/10.1073/pnas.1104651108.

35. **Carrera M, Zandomeni RO, Fitzgibbon J, Sagripanti JL.** 2007. Difference between the spore sizes of *Bacillus anthracis* and other *Bacillus* species. J Appl Microbiol **102:**303–312.

36. **Carrera M, Zandomeni RO, Sagripanti JL.** 2008. Wet and dry density of *Bacillus anthracis* and other *Bacillus* species. J Appl Microbiol **105:**68–77. http://dx.doi.org/10.1111/j.1365-2672.2008.03758.x.

37. **Plomp M, Carroll AM, Setlow P, Malkin AJ.** 2014. Architecture and assembly of the *Bacillus subtilis* spore coat. PLoS One **9:**e108560. http://dx.doi.org/10.1371/journal.pone.0108560.

38. **Eichenberger P, Fujita M, Jensen ST, Conlon EM, Rudner DZ, Wang ST, Ferguson C, Haga K, Sato T, Liu JS, Losick R.** 2004. The program of gene transcription for a single differentiating cell type during sporulation in *Bacillus subtilis*. PLoS Biol **2:**e328. http://dx.doi.org/10.1371/journal.pbio.0020328.

39. **Setlow P.** 2013. Summer meeting 2013—when the sleepers wake: the germination of spores of *Bacillus* species. J Appl Microbiol **115:**1251–1268. http://dx.doi.org/10.1111/jam.12343.

40. **Velásquez J, Schuurman-Wolters G, Birkner JP, Abee T, Poolman B.** 2014. *Bacillus subtilis* spore protein SpoVAC functions as a mechanosensitive channel. Mol Microbiol **92:**813–823. http://dx.doi.org/10.1111/mmi.12591.

41. **Imamura D, Kuwana R, Takamatsu H, Watabe K.** 2011. Proteins involved in formation of the outermost layer of *Bacillus subtilis* spores. J Bacteriol **193:**4075–4080. http://dx.doi.org/10.1128/JB.05310-11.

42. **He LM, Tebo BM.** 1998. Surface charge properties of and Cu(II) adsorption by spores of the marine *Bacillus* sp. strain SG-1. Appl Environ Microbiol **64:**1123–1129.

43. **Chen X, Mahadevan L, Driks A, Sahin O.** 2014. Bacillus spores as building blocks for stimuli-responsive materials and nanogenerators. Nat Nanotechnol **9:**137–141. http://dx.doi.org/10.1038/nnano.2013.290.

44. **McKenney PT, Driks A, Eichenberger P.** 2013. The *Bacillus subtilis* endospore: assembly and functions of the multilayered coat. Nat Rev Microbiol **11:**33–44. http://dx.doi.org/10.1038/nrmicro2921.

45. **Popham DL, Gilmore ME, Setlow P.** 1999. Roles of low-molecular-weight penicillin-binding proteins in *Bacillus subtilis* spore peptidoglycan synthesis and spore properties. J Bacteriol **181:**126–132.

46. **Meador-Parton J, Popham DL.** 2000. Structural analysis of *Bacillus subtilis* spore peptidoglycan during sporulation. J Bacteriol **182:**4491–4499. http://dx.doi.org/10.1128/JB.182.16.4491-4499.2000.